

Photorefractive Keratectomy Using Solid State Laser 213 nm and Excimer Laser 193 nm: A Randomized, Contralateral, Comparative, Experimental Study

Nikolaos S. Tsiklis, George D. Kymionis, George A. Kounis, Irini I. Naoumidi, and Ioannis G. Pallikaris

PURPOSE. To compare histopathologic changes after photorefractive keratectomy (PRK) for myopia using either a solid state laser (SSL) at 213 nm or an excimer laser (EL) at 193 nm in an experimental model.

METHODS. Forty pigmented rabbits (80 eyes) underwent myopic PRK for the correction of 6 D. Photoablation was randomly assigned, with a solid state laser used in one eye and an EL in the fellow eye. Rabbits were killed immediately after ablation ($n = 10$) or at 7 days ($n = 10$), 1 month ($n = 8$), 3 months ($n = 6$), or 12 months ($n = 6$) after surgery. Corneal tissue was preserved for light microscopy and transmission electron microscopy at all postoperative intervals.

RESULTS. All eyes reepithelialized in 1 week with no early or late postoperative complication. Immediately after ablation, light, scanning, and transmission electron microscopy revealed relatively smooth ablation surfaces in both groups. Seven days after surgery, epithelium in the SSL specimens appeared thinner than in the EL specimens. Activated keratocytes were observed adjacent to the epithelium in both groups, whereas endothelial cells demonstrated normal morphology. At 1, 3, and 12 months after surgery, tissue appearance of all corneal layers was similar in both groups.

CONCLUSIONS. PRK in rabbits using ultraviolet SSL and EL revealed similar histopathologic findings up to 1 year after surgery. (*Invest Ophthalmol Vis Sci.* 2008;49:1415-1420) DOI: 10.1167/iovs.07-1280

Excimer laser (EL) using 193 nm light provides precise tissue removal with less collateral damage than it does using longer wavelengths.¹⁻³ Corneal absorption remains strong and relatively stable from 193 to 220 nm⁴; therefore, laser pulses in the far UV region (190-220 nm) can be used for corneal ablation with similar characteristics (ablation threshold, ablation rate, and size of collateral damage zone).

As an alternative source of such UV radiation, researchers used the fifth harmonic of an Nd:YAG laser, which emits at 213 nm wavelength. In vitro⁵ and in vivo⁶ studies with 213-nm solid state laser (SSL) demonstrated smooth ablation surfaces, whereas the clinical course and the histopathologic findings were similar to those of EL photorefractive keratectomy (PRK).⁷

There are a number of theoretical and practical advantages of an SSL compared with an EL system: wavelength closer to absorption peak of corneal collagen and less sensitive to corneal hydration, higher pulse-to-pulse energy stability, smaller spot size, absence of toxic gases, and low maintenance costs. However, only two SSL platforms are commercially available. Whether the theoretical advantages of the SSL platforms compared with the EL systems have any practical impact on corneal healing still must be elucidated.

In this randomized, contralateral, experimental study, we compared histopathologic changes up to 12 months after myopic PRK in rabbits between an SSL of 213-nm wavelength (Pulzar Z1 Laser System; CustomVis, Balcatta, Australia) and a conventional EL system of 193 nm (Allegretto 400 Hz WaveLight Excimer Laser; WaveLight, Inc., Erlangen, Germany) using light microscopy and transmission electron microscopy.

METHODS

Experiments were conducted in accordance with the ARVO Statement for the Use of Animals in Ophthalmic and Vision Research, and the design of the study was approved by the Animal Care Committee. Because of the increased variation among rabbits in corneal wound healing response after refractive surgery (especially after PRK), both eyes of each animal were included in the study.^{8,9} Eighty eyes of 40 pigmented rabbits (of the same sex, weighing 2.5-3.5 kg) were randomly assigned with a flip of a coin to undergo PRK with a 193-nm conventional EL system (Allegretto 400 Hz WaveLight Excimer Laser; WaveLight, Inc.; fluence 180 mJ/cm² per pulse at 10 Hz) in one eye and with a 213-nm wavelength SSL system (Pulzar Z1 Laser System; CustomVis; fluence 180 mJ/cm² per pulse at 10 Hz) in the fellow eye.

Animals were anesthetized by intramuscular injection (mixture of xylazine hydrochloride [5 mg/kg] and ketamine hydrochloride [50 mg/kg]) and draped; an eyelid speculum was used to hold the lids open, and 2 drops of local anesthesia were given. After 2 minutes, mechanical epithelium debridement of the central 7.5 mm of the cornea (previously marked with a 7.5-mm trephine) was performed. Both lasers were programmed for 6 diopters (D) at 5 mm optical zone (0.5-mm transitional zone), and approximately 50 μ m stromal tissue was removed. The ablation area was adjusted to be the same in both eyes. Mean central corneal thickness was measured with an ultrasound pachymeter (Corneo-Gage Plus; Sonogage Inc., Cleveland, OH) before and after epithelium debridement (362.6 μ m [range, 320-455 μ m] and 330.4 μ m [range, 287-430 μ m], respectively). In all eyes, ophthalmic ointment dexamethasone 0.1%/tobramycin 0.3% (Tobradex; Alcon, Fort Worth, TX) was applied 4 times per day until complete reepithelialization.

Each animal was killed immediately after ablation (group 1, $n = 10$), at 7 days (group 2, $n = 10$), or at 1 month (group 3, $n = 8$), 3 months (group 4, $n = 6$), or 12 months (group 5, $n = 6$) after the experiment by an intravenous overdose of pentobarbital. Eyes were enucleated and placed in glutaraldehyde 2.5% in 0.1 M cacodylate buffer (pH 7.3) at 4°C for at least 24 hours and then were postfixed in 1% osmium tetroxide in 0.1 M cacodylate buffer (pH 7.3) at 4°C for 1

From the Department of Ophthalmology, Institute of Vision and Optics, University of Crete Medical School, Heraklion, Crete, Greece.

Submitted for publication October 2, 2007; revised November 29, 2007; accepted February 26, 2008.

Disclosure: N.S. Tsiklis, None; G.D. Kymionis, None; G.A. Kounis, None; I.I. Naoumidi, None; I.G. Pallikaris, None

The publication costs of this article were defrayed in part by page charge payment. This article must therefore be marked "advertisement" in accordance with 18 U.S.C. §1734 solely to indicate this fact.

Corresponding author: Nikolaos S. Tsiklis, Department of Ophthalmology, Institute of Vision and Optics, University of Crete Medical School, 71003 Heraklion, Crete, Greece; ntsiklis@hotmail.com.

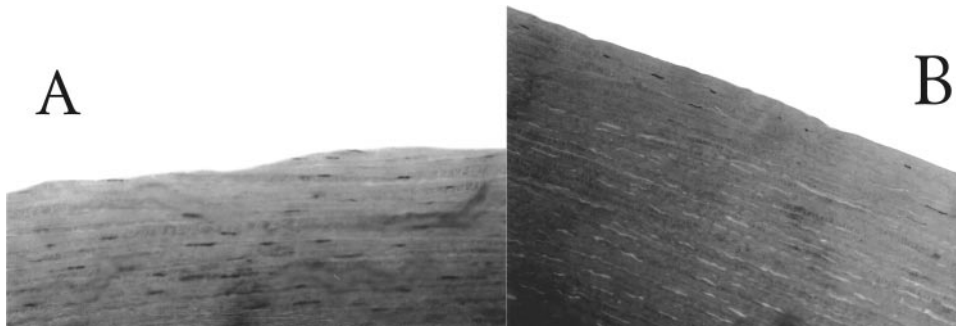


FIGURE 1. Corneal morphology immediately after laser ablation. SSL-ablated (a) and EL-ablated (b) samples demonstrate smooth corneal surface. Light microscopy. Original magnification, $\times 320$.

hour. After dehydration and embedding in epoxy resin, corneal samples were sectioned, stained, and examined using light microscopy. In the areas with mostly pronounced morphologic alterations, electron microscopy was performed. Standard techniques for the preparation of scanning and transmission electron microscopy examination were used. All semithin sections were stained with modified trichrome stain¹⁰; all sections for electron microscopy were stained with uranyl acetate and lead citrate.

RESULTS

All procedures were completed with no complications. Eyes of both groups reepithelialized within 1 week without any sign of corneal inflammation. Subepithelial haze was clinically observed at 7 days after surgery, peaked at 1 month, and then decreased over time.

Light Microscopy

Immediately after the ablation (group 1; Fig. 1), samples of both groups (SSL and EL) demonstrated smooth ablation surface, with no signs of edema or distortion of the adjacent corneal stroma. The structure of the Descemet membrane or the endothelial layer did not differ from that of intact tissues.

Seven days after surgery (group 2; Fig. 2), the epithelium in the SSL specimens appeared two to three layers thinner than in the normal specimens and had reduced numbers of wing cells. Samples of EL eyes demonstrated normal epithelial thickness (five to six layers), or mild hyperplasia. In both groups, activated keratocytes were observed in the stromal layers adjacent to the epithelium. Histologic signs of infiltration or edema were not observed in any specimen. The

structure of endothelial monolayer was similar to that of intact samples, and the endothelial cells demonstrated normal morphology.

One month after laser ablation, the epithelial layer in each group was characterized by virtually normal morphology (Fig. 3). Three months after laser ablation (group 3), the specimens of SSL- and EL-ablated eyes demonstrated a tendency to reduced thickness of the subepithelial fibrous stromal layer. Twelve months after laser ablation (group 4) was the maximum postoperative observation period. In both groups, the thickness of the subepithelial stroma did not exceed 10 to 15 μm . Structure of the epithelium, stroma, and endothelium was identical with that of intact tissues.

Transmission Electron Microscopy

Immediately after ablation in EL and SSL samples, the corneal surface was relatively smooth but had a small number of irregularities distributed almost evenly across the ablation area (Fig. 4), which was covered by a confluent layer of a pseudomembrane without any cracks or holes. The pseudomembrane consisted of an amorphous electron-dense substance with a small number of granular inclusions and sparse vesicle-like structures. The structure of the pseudomembrane was similar in both groups of samples (Fig. 5).

The common characteristic feature of the transmission electron microscopy structure of EL and SSL ablations was flatness of the outer pseudomembrane surface, in contrast to its inner surface (i.e., the transition between the pseudomembrane and the intact-looking stroma). The roughness of this surface was responsible for the irregularity of the pseudomembrane thickness. The pseudomembrane was slightly thicker in the EL-ablated samples than in the SSL-ablated samples.

EL-ablated samples showed keratocyte dehydration to a variable degree, vacuolization, and pronounced fragmentation

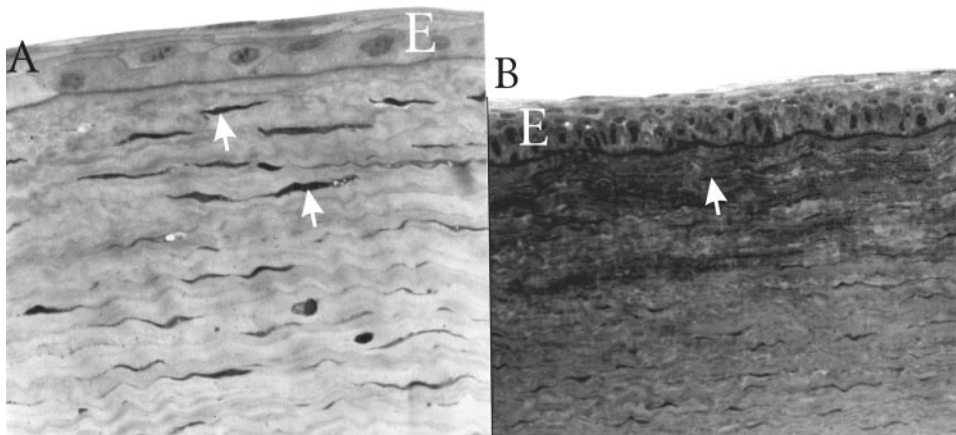


FIGURE 2. Seven days after laser ablation. In the SSL-ablated sample (a), the recovered epithelium (E) demonstrates fewer wing cells than the EL-ablated specimens (b). Note the activated keratocytes (arrowheads) in the upper stroma of the specimens of both groups. Light microscopy. Original magnifications, (a) $\times 500$; (b) $\times 320$.

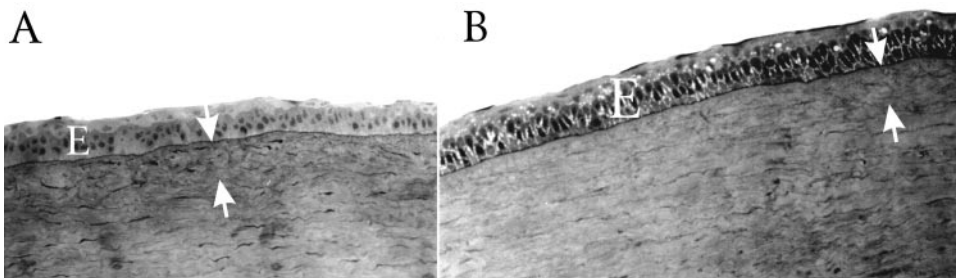


FIGURE 3. One month after laser ablation. Morphologic characteristics of the epithelium over the corneal surface ablated by the SSL (a) and the EL (b) are similar. *Arrowheads:* subepithelial fibrous layer. Light microscopy. Original magnification, $\times 320$.

of the cell bodies. At the same time, the SSL-ablated stroma demonstrated normal appearance of keratocytes across the entire corneal thickness.

The morphology of the deeper corneal layers was similar in all specimens, and keratocytes and extracellular matrix had normal structure. The Descemet membrane and the endothelial layer demonstrated normal appearance, without any sign of edema or loss of intercellular contact (Fig. 6).

Seven days after surgery (group 2), the epithelial layers demonstrated stratification (superficial layers, wing cells, basal cells) in all samples of both groups. In the SSL group, the epithelial cells, in spite of reduced epithelial thickness, showed normal morphologic characteristics (Fig. 7). In both samples (SSL and EL eyes), the basal cells were connected to the basement membrane by a small number of hemidesmosomes distributed irregularly. Activated keratocytes were observed in the upper part of the stroma in SSL and EL eyes.

One month after laser ablation (group 3), the epithelial layer in both samples demonstrated hemidesmosomes regularly distributed between the basal epithelial cells and superficial stroma.

In the specimens of both groups (SSL and EL eyes), a scarred stromal layer was observed under the recovered epithelium. The scarred stromal layer contained a significant number of activated keratocytes; its thickness varied from 20 μm to 30 μm (Fig. 8). This layer was clearly distinguishable above the intact stroma because of chaotically oriented fibrils of different size with numerous amorphous inclusions. Slight vacuolization of this layer was observed, which is mentioned frequently in the descriptions of superficial stroma after PRK procedure. The structure of underlying stroma, Descemet membrane, and endothelium was close to normal.

Three months after surgery (group 4), the corneal epithelium demonstrated normal morphologic characteristics in both groups of specimens. The morphology of subepithelial stroma appeared similar to that observed 1 month after laser ablation, except that the corneal epithelium appeared thicker in comparison with earlier observation periods. In some areas, the specimens of both groups demonstrated splitting or reduplication of the basement membrane.

Twelve months after laser ablation (group 5), the subepithelial layer in the specimens of SSL and EL samples demonstrated a tendency to thinning, without any significant structural alterations. Descemet membrane and endothelium in all samples did not demonstrate any morphologic difference with the intact tissues except for the electron-dense layer inside the Descemet membrane observed in the samples of both groups (Fig. 9).

DISCUSSION

The strong corneal absorption in the far UV region (190–220 nm wavelength) had, as a result, high precision of corneal ablation without damage to the adjacent tissue.⁴

Two main sources of ultraviolet radiation are used in corneal photoablation, the ArF EL (193-nm wavelength) and the fifth harmonic of the Nd:YAG laser (213-nm wavelength). This slightly higher wavelength of the SSL could possibly be associated with a greater penetration depth and larger actinic damage. Moreover, 213-nm wavelength is less sensitive to corneal hydration than 193-nm radiation.¹¹ Thus, corneal hydration¹² and environmental humidity,¹³ factors that could affect the final outcome with the conventional EL systems, are limited with the SSL. Furthermore, SSLs have higher pulse-to-pulse energy stability and smaller

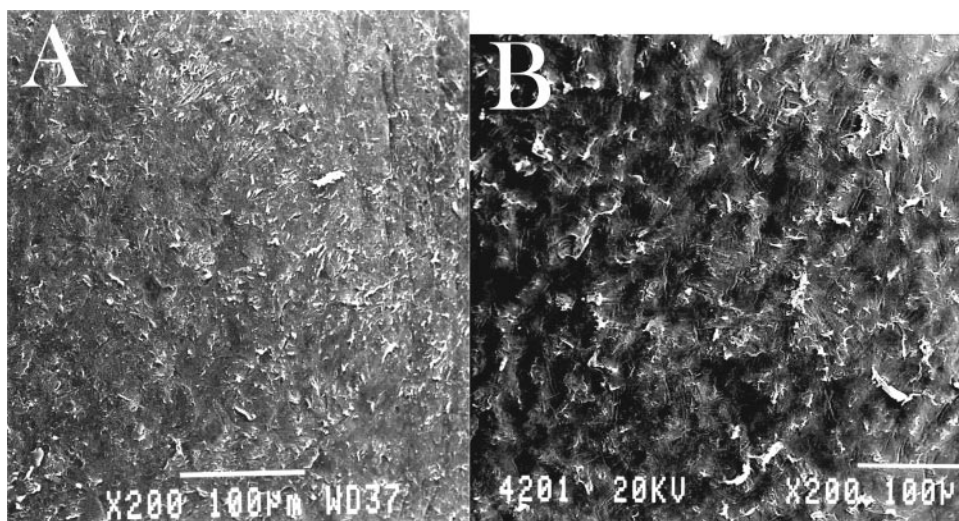


FIGURE 4. Scanning electron microscopy of SSL-ablated (a) and EL-ablated (b) corneal samples immediately after ablation. The superficial stroma in each group looks relatively smooth and has no cracks or holes. Scanning electron microscopy. Original magnification, $\times 200$.

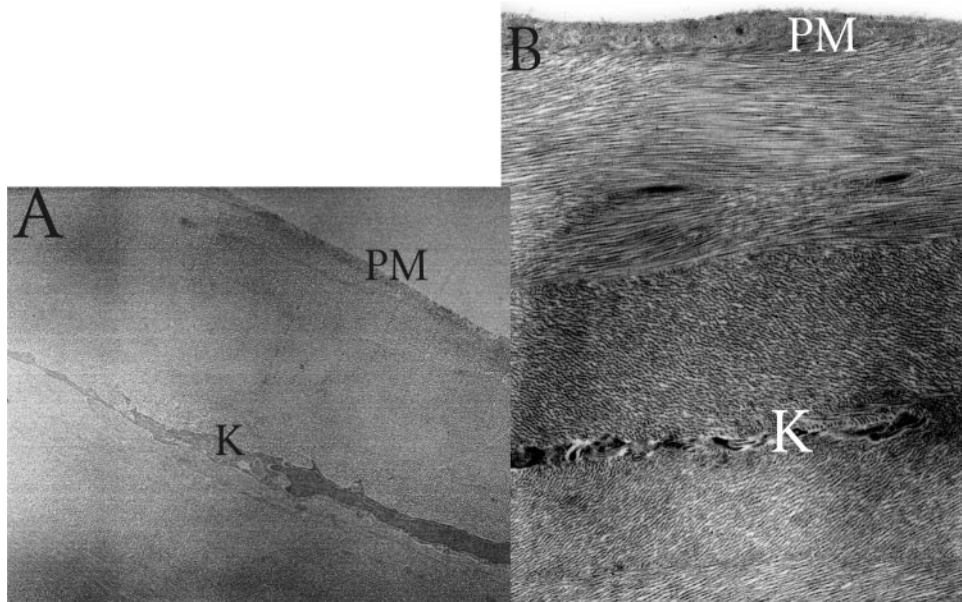


FIGURE 5. Transmission electron microscopy of SSL-ablated (a) and EL-ablated (b) corneal samples immediately after ablation. Pseudomembrane (PM.) on the corneal stroma demonstrates similar structure in both groups. In the upper stroma of EL-ablated samples (b), structural changes of keratocytes (K) were observed, especially fragmentation and vacuolization. Transmission electron microscopy. Original magnifications, (a) $\times 5000$; (b) $\times 6600$.

beam size. The latter minimizes the mechanical stress of the cornea during ablation,¹⁴ a phenomenon that might correlate with endothelial cell changes.¹⁵

The present study showed a smooth ablation surface with no edema or distortion of the adjacent corneal stroma, indicating the absence of thermal damage in both groups (SSL- and EL-treated eyes) immediately after myopic PRK in rabbit eyes. Hemidesmosomes regularly distributed between the basal epithelial cells and superficial stroma 1 month after surgery. The upper stroma contained a significant number of activated keratocytes with slight vacuolization. In all post-operative examinations, the deeper stroma had keratocytes and extracellular matrix of normal structure. The endothelial layer was intact, and endothelial cells appeared

normal in all samples of both groups, a crucial parameter for the safety of the procedure. During the entire 12 months of the study, no sign of corneal mutagenesis (tumor or other corneal abnormality) was seen, even though 213 nm wavelength is closer to the absorption peak of DNA.¹⁶ These results are in accordance with previous experimental studies and confirm normal corneal healing over time, after ablation with 193-nm or 213-nm wavelength irradiation, with no adverse effect in deeper corneal layers.^{5-7,17-19}

There were only few small histologic differences between the two groups. Light microscopy showed that epithelium in the SSL specimens (1 week after surgery) was thinner than normal, whereas the EL group demonstrated normal epithelial thickness with mild hyperplasia. More-

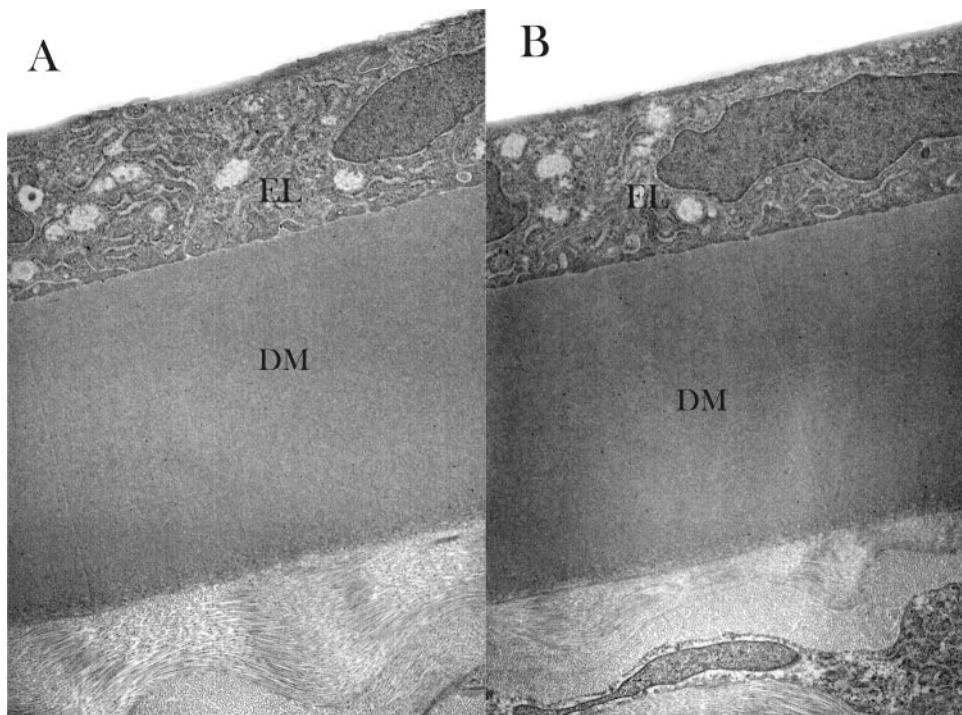


FIGURE 6. Transmission electron microscopy of SSL-ablated (a) and EL-ablated (b) corneal samples immediately after ablation. Descemet membrane (DM) and endothelial layer (EL) have close to normal appearance in each group. Transmission electron microscopy. Original magnification, $\times 5000$.



FIGURE 7. SSL-ablated specimen 7 days after surgery. In spite of the recovered integrity of corneal epithelium (E), the number of epithelial layers is reduced in comparison to normal. Note the extremely few hemidesmosomes (*arrowheads*). Transmission electron microscopy. Original magnification, $\times 3000$.

over, although the pseudomembrane as viewed with transmission electron microscopy had a similar structure without any cracks or holes in either group, it was slightly thicker in the EL specimens.

In contrast, the histopathologic study of Ren et al.⁶ revealed epithelial thickening and hyperplasia 10 days after PRK with 213-nm wavelength in rabbit corneas after light microscopy examination. This difference might have resulted from different laser parameters (fluence, ablation rate, spot size) or different attempted corrections. There is an especially limited literature on histologic changes after corneal ablation using the 213-wavelength though the results of the studies are not directly comparable.^{3,6,17,20} Moreover, even though it seems that 213 nm irradiation does not induce thermal damage,²⁰ little is known about mechanical stress caused by the pressure wave and secondary (fluorescence) radiation.

The observed differences in the healing process after corneal ablation with 193- and 213-nm wavelength are unlikely to have had any practical impact on visual outcome; in addition, all the published clinical data after refractive surgery in humans with SSLs are promising and comparable with those of EL systems of 193-nm wavelength.^{19,21-24}

Potential limitations are apparent in this study. The limited number of subjects, the absence of a quantitative and

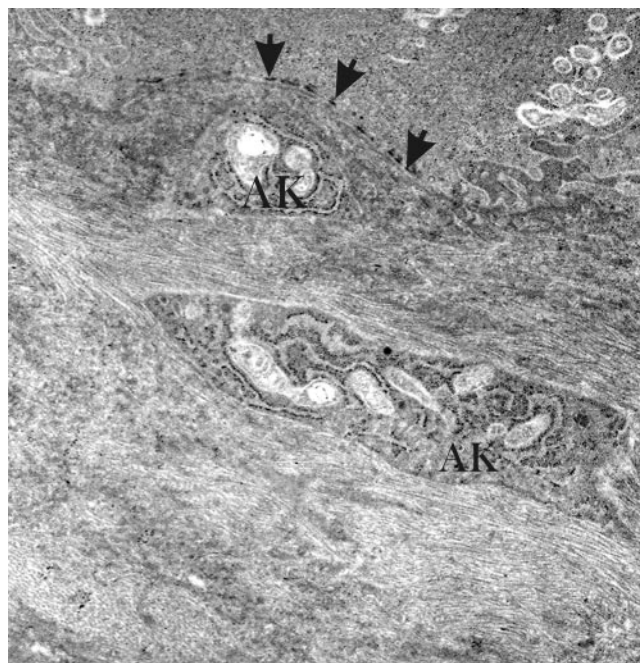


FIGURE 8. SSL-ablated specimen 1 month after surgery. The epithelium is connected to the stroma by significant numbers of mature hemidesmosomes (*arrowheads*). The upper stromal layer consists of chaotically oriented fibrous material and numerous activated keratocytes (AK). Transmission electron microscopy. Original magnification, $\times 6600$.

immunohistochemistry analysis, the small fluence differences between the two lasers, the standard attempted correction, and the possible difference in the pathophysiological behavior of the rabbit and the human eye are the major ones.

Future experimental and human (with confocal microscopy analysis) prospective studies, including more eyes in a large range of attempted corrections, are needed to clarify any differences between the two laser platforms.

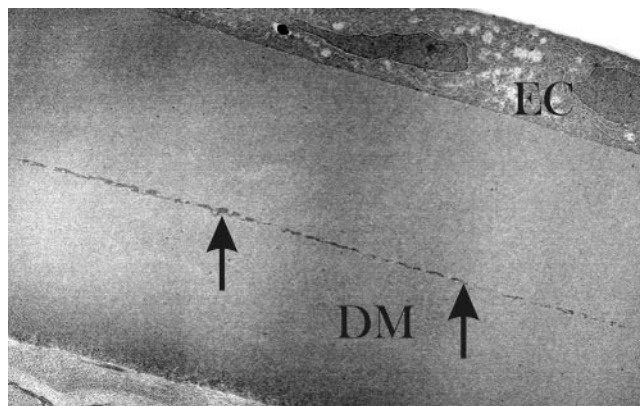


FIGURE 9. SSL-ablated specimen 12 months after surgery. A characteristic electron-dense layer (*arrowheads*) was observed within the Descemet membrane (DM) of many SSL-ablated samples. At the same time, the endothelial cells (EC) had normal appearance. Transmission electron microscopy. Original magnification, $\times 3000$.

References

1. Trokel SL, Srinivasan R, Braren B. Excimer laser surgery of the cornea. *Am J Ophthalmol*. 1983;96:710.
2. Ren Q, Gailitis P, Thompson KP, Lin JT. Ablation of the cornea and synthetic polymers using a UV (213nm) solid state laser. *IEEE J Quantum Electron*. 1990;26:2284-2288.
3. Gailitis RP, Ren QS, Thompson KP, et al. Solid state ultraviolet laser (213 nm) ablation of the cornea and synthetic collagen lenticules. *Laser Surg Med*. 1991;11:556-562.
4. Lembares A, Hu XH, Kalmus GW. Absorption spectra of corneas in the far ultraviolet region. *Invest Ophthalmol Vis Sci*. 1997;38:1283-1287.
5. Ren Q, Simon G, Parel JM. Ultraviolet solid-state laser (213-nm) photorefractive keratectomy: in vitro study. *Ophthalmology*. 1993;100:1828-1834.
6. Ren Q, Simon G, Legeais JM, et al. Ultraviolet solid-state laser (213-nm) photorefractive keratectomy: in vivo study. *Ophthalmology*. 1994;101:883-889.
7. L'Esperance FA Jr, Taylor DM, Warner JW. Human excimer laser keratectomy: short-term histopathology. *J Refract Surg*. 1988;4:118-124.
8. Nwanegbo EC, Romanowski EG, Gordon YJ, Gambotto A. Efficacy of topical immunoglobulins against experimental adenoviral ocular infection. *Invest Ophthalmol Vis Sci*. 2007;48:4171-4176.
9. Donnenfeld RS, Perry HD, Solomon R, et al. A comparison of gatifloxacin to ciprofloxacin in the prophylaxis of streptococcus pneumonia in rabbits in a LASIK model. *Eye Contact Lens*. 2006;32:46-50.
10. Rock ME, Anderson JA, Binder PS. A modified trichrome stain for light microscopic examination of plastic-embedded corneal tissue. *Cornea*. 1993;12:255-260.
11. Dair GT, Ashman RA, Eikelboom RH, et al. Absorption of 193- and 213-nm laser wavelengths in sodium chloride solution and balanced salt solution. *Arch Ophthalmol*. 2001;119:533-537.
12. Dougherty PJ, Wellish KL, Maloney RK. Excimer laser ablation rate and corneal hydration. *Am J Ophthalmol*. 1994;118:169-176.
13. Walter AK, Stevenson WA. Effect of environmental factors on myopic LASIK enhancement rate. *J Cataract Refract Surg*. 2004;30:798-803.
14. Krueger RR, Seiler T, Gruchman T, et al. Stress wave amplitudes during laser surgery of the cornea. *Ophthalmology*. 2001;108:1070-1074.
15. Gomez IP, Efron N. Change to corneal morphology after refractive surgery (myopic laser in situ keratomileusis) as viewed with confocal microscopy. *Optom Vis Sci*. 2003;80:690-697.
16. Marshall J, Trokel S, Rothery S, Krueger RR. Photoablative reprofiling of the cornea using an excimer laser: photorefractive keratectomy. *Lasers Ophthalmol*. 1986;1:21-48.
17. Caughey TA, Cheng F-C, Trokel SL, et al. An investigation of laser tissue interaction of a 213nm laser beam with animal corneas. *Lasers Light Ophthalmol*. 1994;6:77-85.
18. Krueger RR, Trokel SL, Schubert HD. Interaction of ultraviolet laser light with the cornea. *Invest Ophthalmol Vis Sci*. 1985;26:1455-1464.
19. Tsiklis NS, Kymionis GD, Pallikaris AI. Endothelial cell density after photorefractive keratectomy for moderate myopia using a 213 nm solid-state laser system. *J Cataract Refract Surg*. 2007;33:1866-1870.
20. Van Saarloos PP, Rodger J. Histological changes and unscheduled DNA synthesis in the rabbit cornea following 213-nm, 193-nm, and 266-nm irradiation. *J Refract Surg*. 2007;23:477-481.
21. Anderson I, Sanders DR, van Saarloos P, Ardrey WJ 4th. Treatment of irregular astigmatism with a 213 nm solid-state, diode-pumped neodymium:YAG ablative laser. *J Cataract Refract Surg*. 2004;30:2145-2151.
22. Roszkowska AM, Korn G, Lenzner M, et al. Experimental and clinical investigation of efficiency and ablation profiles of new solid-state deep-ultraviolet laser for vision correction. *J Cataract Refract Surg*. 2004;30:2536-2542.
23. Roszkowska AM, De Grazia L, Ferreri P, Ferreri G. One-year clinical results of photorefractive keratectomy with a solid-state laser for refractive surgery. *J Refract Surg*. 2006;22:611-613.
24. Tsiklis NS, Kymionis GD, Kounis GA. One-year results of photorefractive keratectomy and laser in situ keratomileusis for myopia using a 213 nm wavelength solid-state laser. *J Cataract Refract Surg*. 2007;33:971-977.